THE ASTROPHYSICAL JOURNAL, 336:722–733, 1989 January 15

X-RAY OBSERVATIONS OF THE STARBURST GALAXY M82

R. SCHAAF,[1,2] W. PIETSCH,[3] P. L. BIERMANN,[2] P. P. KRONBERG,[4] AND T. SCHMUTZLER[2,5]
Received 1987 August 17; accepted 1988 June 21

ABSTRACT

We report here on long ($\sim 10^5$ s) X-ray observations of the starburst galaxy M82 with the European X-ray satellite *EXOSAT*. The observations with the low-energy imaging instrument confirm that there is extended X-ray emission from above and below the disk, with an overall extent perpendicular to the disk of almost 6′ corresponding to 6 kpc. We present one of the best defined X-ray spectra yet of a starburst galaxy. The medium energy instrument measurements can be fitted with a power-law spectrum, consistent with inverse Compton emission, or with thermal emission from optically thin hot gas of a temperature of 9^{+9}_{-4} keV. Using, in addition, the earlier *Einstein* HRI and MPC observations, we discuss the possible origin of the X-ray emission.

Subject headings: galaxies: individual (M82) — galaxies: X-rays — stars: formation

I. INTRODUCTION

Messier 82 has become a prototype for starburst galaxies, which as a class are now readily identifiable in the data from the far-infrared satellite *IRAS*. M82 is of particular interest because of its relative proximity, which permits the observation of individual star-related radio sources (cf. Kronberg, Biermann, and Schwab 1985). It has, further, been recently possible to gather initial data on the temporal evolution of individual supernova remnants and other energetic objects (Kronberg and Sramek 1985). These have recently provided a first-order confirmation by direct statistics of the high rate of star formation (Rieke *et al.* 1980).

M82 has already been shown, from *Einstein* X-ray satellite data to exhibit huge X-ray plumes perpendicular to the disk (Watson, Stanger, and Griffiths 1984; Kronberg, Biermann, and Schwab 1985). CO emission line observations (Sofue *et al.* 1986) support the interpretation of the X-ray plumes as outflow from the disk. Being also a classic infrared excess galaxy (cf. Soifer *et al.* 1986) the detailed study offered by its proximity will elucidate the origin of the large energy release in the FIR. We note that X-ray absorption is likely to be strong in those regions emitting FIR light from hot dust.

Because of this strong and general interest in M82, we observed it with *EXOSAT* for a total of 28 hr. We present the data and discuss their significance for the physical conditions and emission mechanisms.

II. OBSERVATIONS

a) General

M82 was observed twice by *EXOSAT*, first on Christmas eve of 1983, and again on 1984 April 10. The details of the observations are given in Table 1. Tables 2 and 3 give other X-ray observations of the M81/M82 region. For a description of the satellite, see Taylor *et al.* (1981).

We have analyzed the low-energy telescope data (LE, 0.06–2.0 keV with the thin lexan filter; de Korte *et al.*, 1981) at ESOC, Darmstadt, as well as at Bonn with the help of Dr. B. Aschenbach (MPE, Garching), and the medium-energy data (ME, 1–15 keV for the argon chamber; Turner, Smith, and Zimmermann 1981) at the Max-Planck-Institut für extraterrestrische Physik, Garching. The LE data from both observations were combined to yield 102,199 s of effective observing time, and the results are shown in Figures 1, 2, and 3, overlaid on an [O II] emission photo (courtesy Dr. H. C. Arp). Figure 1 is smoothed with a 20″ Gaussian, Figure 2 with a 40″ Gaussian to show weaker more extended features, and in Figure 3 with a 4″ Gaussian to show the weak point source.

For the LE-analysis a background observation (days 230–232, 1984, thin lexan filter, duration 231,847 s) was smoothed with a two-dimensional Gaussian of 1′.6 width to produce a flat field. In an area outside of a circle of 10′ radius around the center of M82 the background field and the two M82 fields were scaled and subtracted, respectively. Residuals from long-wavelength spatial patterns in the fields were $\lesssim 10^{-2}$ counts per pixel (1 pixel = 4″ × 4″) for the long M82 observations, and $\lesssim 6 \times 10^{-3}$ counts per pixel for the short observation. After subtraction the fields were rotated and added. The background around M82 in an area of 12′ × 8′ is consistently higher than farther out; however, due to long-wavelength spatial variations in the outermost reference regions this local background is only significant at the 1 σ level and is therefore ignored in the following. The count rate of M82 above this local background is $(1.5 \pm 0.1)\ 10^{-2}$ counts s^{-1} corrected for sampling dead time and vignetting.

The LE observations confirm the earlier result that the X-ray emission from M82 *extends far above and below the disk.* The image in Figure 2 is about 4′ by 6′ (smoothed with a 40″ Gaussian). It is thus as extensive as the earlier *Einstein* HRI image. The LE emission appears to cover well the region of the optical emission filaments, which are stronger in the south where the high-resolution image shows a fair amount of emission close to the galaxy and thus independently confirms the earlier *Einstein* result. This confirmation is interesting since the LE instrument has more of its sensitivity in the very soft X-ray range than the HRI of *Einstein.*

The ME data presented a special problem in the analysis, because of the difficulty in accurately determining the background. Only after the first year of the mission for observations of faint sources was *EXOSAT* routinely operated with half of the ME detectors mechanically offset by 2° in order to obtain

[1] Astronomische Institute der Universität Bonn.
[2] Max-Planck-Institut für Radioastronomie, Bonn.
[3] Max-Planck-Institut für Physik und Astrophysik, Garching.
[4] University of Toronto, Department of Astronomy.
[5] Max-Planck-Institut für Kernphysik, Heidelberg.

TABLE 1

EXOSAT OBSERVATIONS OF M82

PARAMETER	DAY OF OBSERVATION	
	358 and 359 (1983)	101 (1984)
Telescope:		
Focal plane detector	CMA	CMA
Start (UT)	$19^h23^m54^s$ (358)	$06^h27^m28^s$ (101)
End (UT)	$16^h26^m02^s$ (359)	$16^h09^m44^s$ (101)
Filter used	Thin lexan	Thin lexan
Effective observing time (s)	69764 s	32435 s
Medium Energy Experiment:		
Spectrum integration		
Start	$18^h26^m00^s$ (358)	$06^h08^m10^s$ (101)
End	$19^h31^m37^s$ (358)	$7^h06^m50^s$ (101)
Start	$15^h51^m05^s$ (359)	...
End	$16^h38^m16^s$ (359)	...
Effective accumulation time (s)	5653	3520
Collimator-efficiency M82[a]	0.96	0.98
Collimator-efficiency M81[a]	0.31	0.18

[a] Pointing at the position of the radio source 41.9 + 58 in M82. This means that the total emission seen includes about 25% (day 358/359, 1983) or about 15% (day 101, 1984), respectively, from M81 assuming equal luminosities for both M81 and M82. Should M81 be brighter than M82 at the epochs of observations, then its contribution is correspondingly larger.

simultaneous source and background measurements. The offset detectors then were exchanged every 3 hr. This proved to allow a good background reduction. The ME observing strategy was different since the optimal strategy during the M82 observations had not yet been established due to problems with one offset motor. For these observations only background data obtained during the change of pointing direction (slew) from the previous target to M82 and during the slew to the next target are available. This slew background may be rather variable and can differ considerably from the background at the source location. The quality of the background reduction can be checked in the high pulse height analyzer (PHA) channels where no source counts are expected and the residual count rate from the source after subtracting background should be consistent with zero flux. If the background subtraction has problems, there will be significant regions of negative counts.

During the observation of 1983 December 24/25 the slews to and from the source were carried out with all ME detectors co-aligned. However the observations of the source itself were performed mostly in an offset configuration with half the detectors pointing to background and unfortunately no exchange of the offset detectors. Therefore, in this observation only a short time at the beginning and end of the observation when the detectors were co-aligned could be used to generate a spectrum by subtracting slew background obtained shortly before and after the source observation. Due to the specific data transmission mode only PHA channels 5–68 of the ME argon counter are available and two channels are always combined.

On 1984 April 10, background is again determined by a slew to the source. Since there was a change in background during the observation and no slew data off the source are available, spectral analysis could be performed only in the beginning of the observation. The data transmission mode gives all 128 PHA channels of the ME argon counter.

Table 1 gives start and end times of integration as well as effective accumulation times for the spectra obtained for the two observations; Figure 4 shows the background subtracted PHA spectra. The difference in the counts s^{-1} observed reflects the fact that in the observation of 1983 December 24/25 (Fig. 4*a*), the flux of all detectors always had two PHA channels added together, whereas on 1984 April 10 (Fig. 4*b*), fluxes in individual PHA channels for only half the detectors are plotted. The plots do not show significant regions of negative counts, indicating that the background could be subtracted reliably.

To further explore possible problems with the ME data, we searched for time variability. Such variability would be an indication of contamination from M81. The energy interval 1.4 to 6

TABLE 2

Einstein MPC OBSERVATIONS OF M82 AND M81

SEQUENCE NUMBER	DAY OF 1979	PRIMARY TARGET	COLLIMATOR EFFICIENCIES		COUNT RATE IN CHANNELS 1–4
			M82	M81	
466	98	M82	1.000	0.180	0.63 ± 0.05
2102	117	M81	0.163	1.000	0.50 ± 0.05
586	123	M82	1.000	0.162	0.77 ± 0.05
585(1)	123	M81	0.156	1.000	0.51 ± 0.05
585(2)	270	M81	0.174	1.000	0.73 ± 0.04
2103	278	M81	0.174	1.000	0.74 ± 0.07

NOTE.—The serendipitous observation (sequence number 3837, day 112, 1979) is not included here.

TABLE 3

Einstein MPC COUNT RATE FOR M81[a]

Sequence Number	Day of 1979	M81 Count Rate Channels 1–4
466	98	≤0.47
2102	117	0.38 ± 0.05
586/585(1)	123	0.40 ± 0.05
585(2)	270	0.61 ± 0.04
2103	278	0.62 ± 0.07

[a] Assuming M82 to be constant.

FIG. 1.—LE emission from M82, smoothed with a 20″ Gaussian and overlaid on an [O II] emission-line photo (courtesy Dr. H. C. Arp). The contour levels are 3, 4, 5, . . . , 10, 15, . . . , 35 σ above a background of 0.007 counts per pixel, corresponding to 0.193, 0.255, 0.317, . . . , 0.627, 0.937, . . . , 2.177 counts per pixel. A pixel is 4″ × 4″.

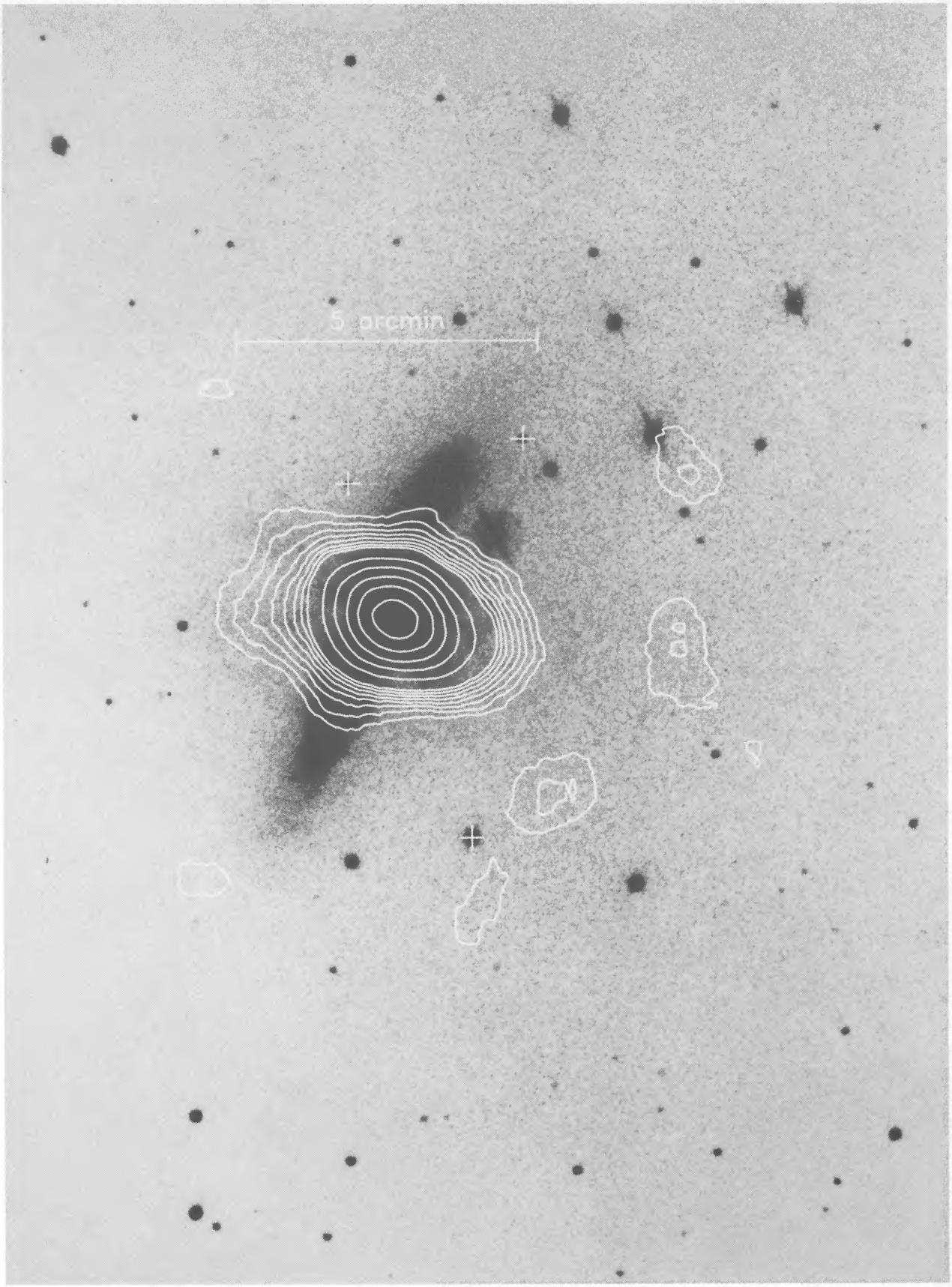

FIG. 2.—The same with the X-ray data smoothed with a 40″ Gaussian to show more extended features. The contour levels are 3, 4, 5, . . . , 10, 15, 20, . . . , 35 σ above a background of 0.007 counts per pixel, corresponding to 0.121, 0.159, . . . , 0.387, 0.577, 0.767, . . . , 1.337 counts per pixel.

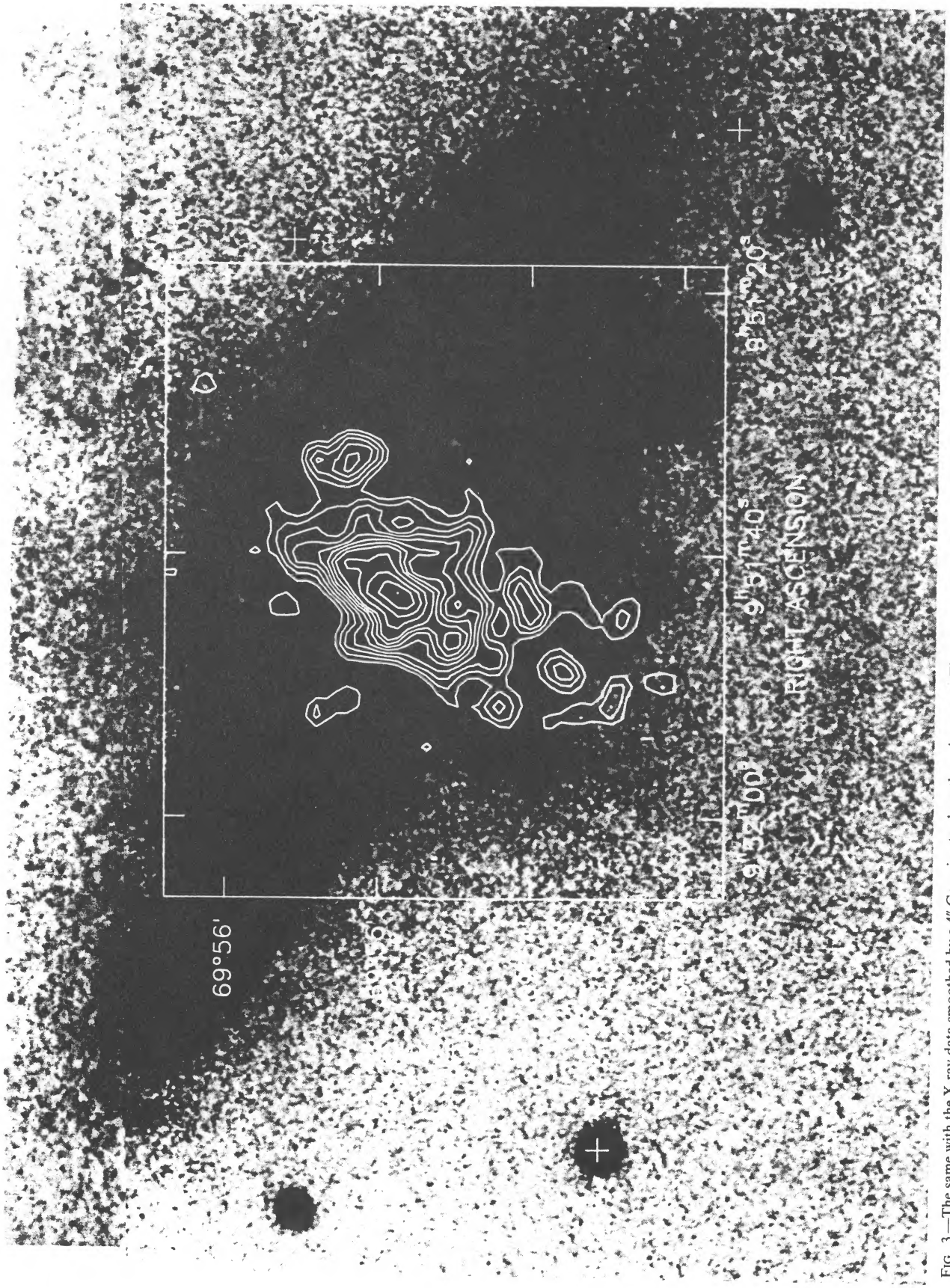

FIG. 3.—The same with the X-ray data smoothed by a 4″ Gaussian to show the point source. The contour levels are 3, 4, 5, ..., 10, 12, 14, 16 and 18 σ above local background of 0.07 counts per pixel, corresponding to 0.91, 1.19, 1.47, ..., 2.87, 3.43, 3.99, 4.55, 5.11 counts per pixel. The strong point source is about 1′ northwest of the X-ray center, at $09^h51^m32^s.9 \pm 0^s.8$, $69°55'12'' \pm 4''$ (1 σ).

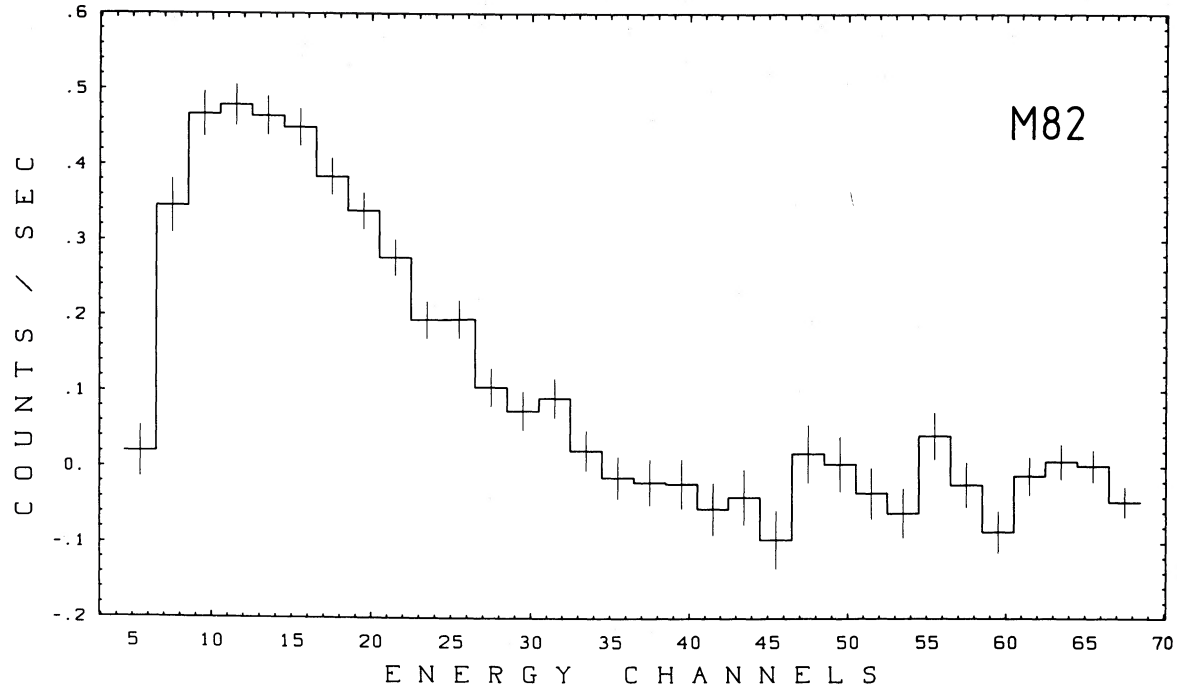

FIG. 4*a*

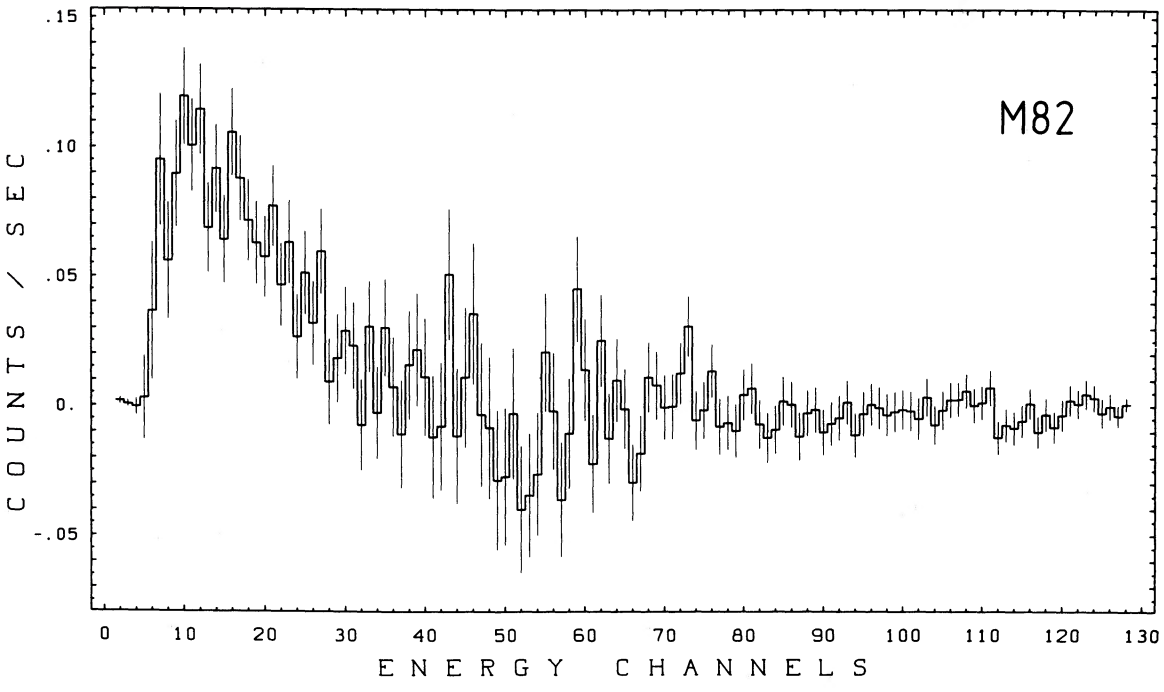

FIG. 4*b*

FIG. 4.—Background subtracted PHA spectra of M82 on 1983 December 24/25 (*a*) and 1984 April 10 (*b*).

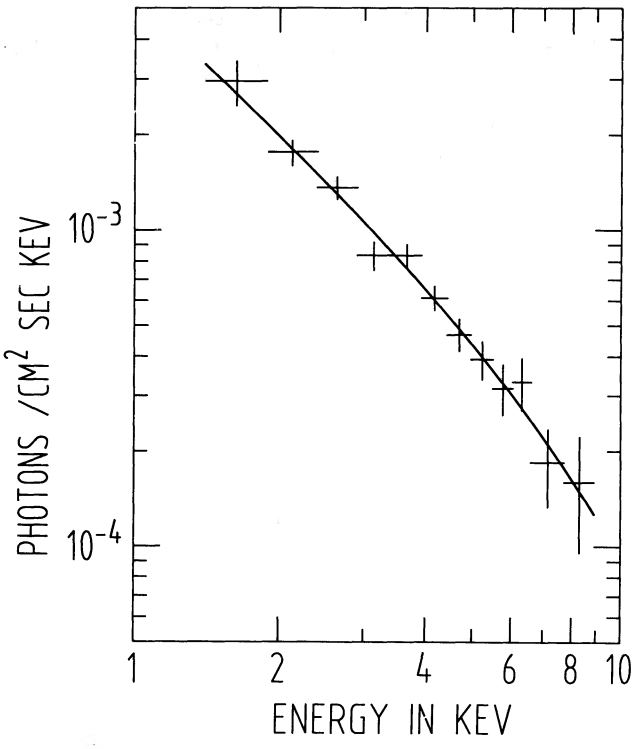

FIG. 5*a*

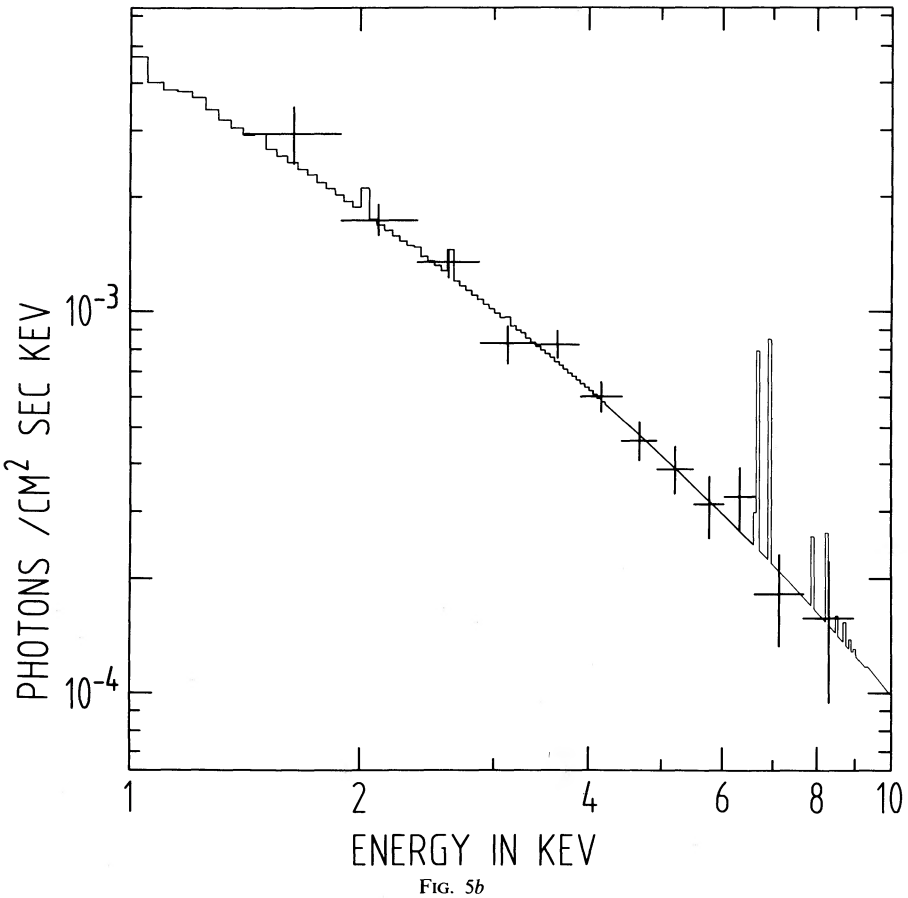

FIG. 5*b*

FIG. 5.—(*a*) Deconvolved ME spectrum of M82 on 1983 December 24/25 assuming a thermal bremsstrahlung model (see Table 4) with the best fitting spectrum. (*b*) A theoretical fit to the ME spectrum using a model including all relevant emission lines; the fit is for a temperature of 9 keV and an absorption column density of 1.0×10^{21} cm^{-2}.

keV, (see Fig. 5*a*) where the instrument is most sensitive, was used to search for time variability. To correct for background changes, the simultaneous offset-half count rates were scaled to the source-half. The scaling factor was determined from the slew to the source of the 1984 April 10 observation. Figure 6 shows the time behavior of the source. While the source intensity was constant during the first observation, during the second observation there is an indication of a 20% increase within the 10 hr of observation. However, since there is no slew information after the observation, it is conceivable that the variability could be due to problems in background subtraction. We note that M81 contributes about 15% to this emission; should M81 have flared by a factor of 2 on time scales of several hours, it would have produced the marginally significant variability observed. Analysis of the earlier *Einstein* MPC observations suggests that M81 contributes at most $\sim$20% to the total emission seen in the ME range (see below), unless M81 had flared considerably beyond any of the earlier flux levels. Given that M82 is free of variability and that the M81 contribution is small, it is useful to discuss the spectrum observed.

The *EXOSAT* (ME) spectrum can be fitted both by a power law (possibly due to inverse Compton radiation) and thermal emission by hot gas. Power law and thermal bremsstrahlung fit parameters are given in Table 4. The deconvolved spectral data for 1983 December 24/25 assuming a thermal bremsstrahlung model are shown in Figure 5*a* together with the best-fitting model spectrum. Corresponding fits to the *Einstein*-MPC data have also been carried out. These give a low column density ($\sim 10^{21}$ cm^{-2}), a photon spectral index of $\sim$2.0, and a normalization factor, C_N, of $\sim 4 \times 10^{-4}$ cm^{-2} s^{-1}, in agreement with the numbers derived here. The total ME X-ray luminosity in the band from 1.4 to 8.9 keV is 3.2×10^{40} ergs s^{-1} (adopting 3.25 Mpc as the distance to M82).

b) Other X-Ray Observations

In order to compare our *EXOSAT* ME-data with earlier observations we obtained (thanks to Dr. F. D. Seward at CfA) the *Einstein* MPC data for all observations of the M82/M81 area. Table 2 gives the observing log, and the count rates obtained: since there are problems with strong background in

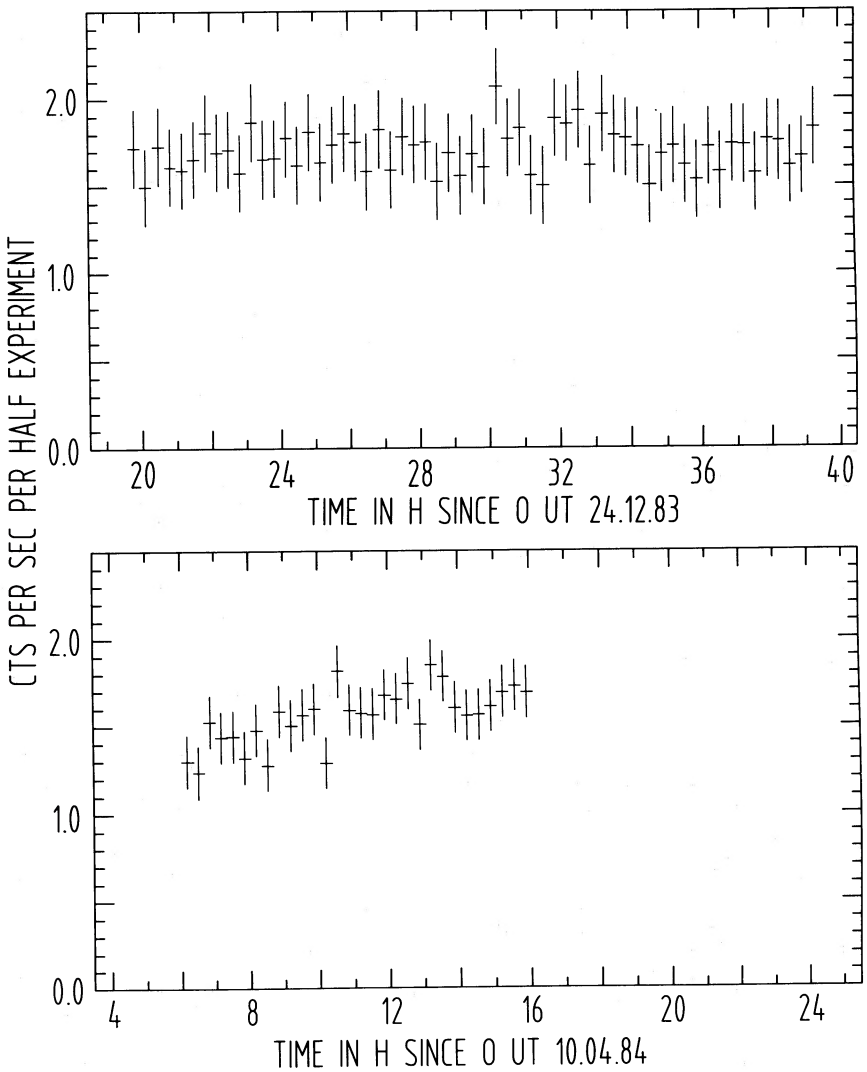

FIG. 6.—ME count rates (1.4–6 keV) integrated for 20 minute intervals (see text)

TABLE 4

FITS TO THE *EXOSAT* ME X-RAY SPECTRA FOR THE POINTINGS AT M82[a]

Parameter	24.12.83	10.4.84
Power Law:		
χ_{red}^2	0.72	0.29
N_H (10^{21} cm^{-2})	<10	<11
C_N[c] 10^{-4} cm^{-2} s^{-1}	$6.3^{+0.8}_{-0.6}$	$4.7^{+0.9}_{-0.7}$
α (photon index)	$1.8^{+0.45}_{-0.30}$	$1.7^{+0.6}_{-0.3}$
Thermal Bremsstrahlung (line emission not included in the fit in Fig. 5*a*):		
χ_{red}^2	0.70[b]	0.40
N_H (10^{21} cm^{-2})	<5.5	<7
C_N[c] (10^{-4} cm^{-2} s^{-1})	$6.4^{+0.8}_{-0.6}$	$4.8^{+0.9}_{-0.6}$
kT (keV)	9^{+9}_{-4}	>4.5

[a] 2σ errors.

[b] Fit in Fig. 5*a* ($N_H = 0$ cm^{-2}, $kT = 9$ keV, $C_N = 6.4 \times 10^{-4}$ cm^{-2} s^{-1}).

[c] C_N is the normalizing factor of the spectrum in which the energy E is normalized to 4 keV.

the high energy channels, we limited ourselves to 1.2–4.9 keV energy. Since the observations on day 123, 1979 for both galaxies strongly overlap in time, we assume that neither M81 nor M82 have varied during the observation sequences 586 and 585(1), and we can thus obtain *individual* count rates: this calculation gives 0.71 ± 0.05 counts s^{-1} for M82 and 0.40 ± 0.05 counts s^{-1} for M81. These numbers can be compared with the count rate given by Watson, Stanger, and Griffiths (1984) of 0.39 ± 0.04 counts s^{-1} for M82 (observation sequences 466 and 586) and by Elvis and van Speybroeck (1982) of 0.38 ± 0.06 counts s^{-1} for M81 [observation sequence 585(1)]. The source of the disagreement with Watson, Stanger, and Griffiths (1984) is not clear. Different energy bands used, time variability, and the reprocessing of the MPC data which now allows the background to be determined with much greater accuracy, all might contribute to discrepancies. Since M82 is not dominated by a single point source (as shown by the HRI observations), it appears unlikely that M82 varied with time. Hence, we can test for temporal variations in the count rate of M81. The result, given in Table 3, clearly shows evidence of moderate variability with time scales of a few months. Barr and Giommi (1985*a*, *b*) in recent *EXOSAT* observations of M81 detect variability: they find M81 to be much brighter, by about a factor of 3, than at the epoch of the *Einstein* observations. In two independent observations, separated by about a month, they find the overall flux of M81 to be about the same, but repeated rapid variations by a factor of 2 on time scales of hours are consistent with the marginally significant variability seen in Figure 6. It follows that a small amount of contamination of the M82 emission by M81, as observed with the ME, by M81 cannot be entirely excluded. The yet earlier X-ray observations of M81 and M82 by other instruments give results consistent with those derived here.

c) *The Source at* $09^h51^m32^s$, $+69°55'7''$

The high-resolution *Einstein* X-ray observations (Watson, Stanger, and Griffiths 1984) showed a strong pointlike source at the position $09^h51^m32^s$, $+6°55'7''$. Figure 3 shows the source in an overlay, using the *EXOSAT* observations. Including a serendipitous *Einstein* observation of M82 on day 112, 1979, we have available four epochs of X-ray observations of M82 with sufficient spatial resolution to observe this source: 1979, day 112; 1979, day 123–126; 1983, day 358; 1984, day 101. The first two observations were made with the *Einstein* satellite (HRI), the latter two with *EXOSAT* (LE). Lacking signal-to-noise ratios, we have to combine the two *EXOSAT* observations to obtain a count rate for the source. For the three independent observations, the count rates are $12. \pm 1.7 \times 10^{-3}$, $7. \pm 1. \times 10^{-3}$ and $4.9 \pm 1.6 \times 10^{-4}$ counts s^{-1}. The positions of the source obtained from the three observations are consistent to about 5″. This source is likely to be a "classic" X-ray binary source, as suggested by its luminosity (Watson, Stanger, and Griffiths 1984).

III. DISCUSSION

In the following we will discuss two possible explanations for the X-ray emission in M82: extended hot gas and inverse Compton emission.

a) *Extended Hot Gas*

Fitting the ME spectrum with emission from hot gas yields a temperature of 9^{+9}_{-4} keV, in agreement with Watson, Stanger, and Griffiths (1984) and also the recent analysis by Fabbiano (1988). A fit with a simple bremsstrahlung spectrum is shown in Figure 5*a*. More detailed fits, with all required emission lines included, give the same temperature range. One of the detailed fits with a theoretical high resolution spectrum (50 eV) is shown in Figure 5*b*. For this fit we have compared Galactic absorption column densities of 0, 1., 3., and 5.5×10^{21} cm^{-2}, and a range of temperatures around 9 keV. The fit shown is for 1.0×10^{21} cm^{-2} column density and 9 keV. The dominant emission lines visible in this theoretical spectrum are Si XIV (2.01 keV), S XVI (2.62 keV), Fe XXV (6.63 and 6.70 keV), Fe XXVI (6.93 keV), Fe XXV (7.90 keV), Fe XXV (8.21 keV), and Fe XXVI (also at 8.21 keV). The abundances used here (both for emission and Galactic absorption) were taken from Allen (1973) with iron arbitrarily reduced by a factor of 2 for the emission in order to obtain a weaker iron line emission contribution. The fact that we do not see definite iron line emission in the ME data is likely due to a combination of the following reasons: (1) the low-energy resolution of the ME instrument, which causes smearing; (2) a possibly lower than normal heavy element abundance in M82, an irregular galaxy; and (3) a possible additional X-ray continuum contribution from another emission mechanism, e.g., inverse Compton emission (see below). From the fit in Figure 5 with a thermal model, we can derive a value of 3.2×10^{63} cm^{-3} for the product of volume, electron density squared and volume filling factor. This value is used in the following section.

All these fits assume a homogeneous source of emission, which is clearly an oversimplification of the true X-ray distribution. The low-energy end of the spectrum is subject to an additional uncertainty in the Galactic absorption; at the high-energy end we suffer from limited photon number statistics.

The observed extent of the low energy emission (Fig. 2) indicates an emitting volume of about 3 kpc diameter for the hot gas. From this and the spectral fit determined above, we can derive a density of $0.27 f_{0.1}{}^{-1/2}$ cm^{-3}, where f is the volume filling factor. We use $f = 0.1$ for reference and write $f_{0.1} = f/0.1$. The pressure is $\sim 7 \times 10^{-9} f_{0.1}{}^{-1/2}$ dyn cm^{-2}, in agreement with the pressure derived from radio observations and the minimum energy argument for a filling factor $f \sim 1$. The cooling time is $1.8 \times 10^8 f_{0.1}{}^{1/2}$ yr, the thermal energy content is $4.8 \times 10^{56} f_{0.1}{}^{1/2}$ ergs, and the mass of hot gas is $1.1 \times 10^7 f_{0.1}{}^{1/2}\ M_\odot$. These numbers match remarkably well with what is expected from a large number of old supernova rem-

nants, provided that the gas could escape from the disk before complete cooling. The cooling time is comparable to the estimated timescale of the starburst itself (Rieke *et al.* 1980; Kronberg, Biermann, and Schwab 1985), and the total amount of hot gas is comparable to the total amount of gas expelled by the 10^{6-7} supernovae expected over the lifetime of the starburst. In the following we shall examine whether the hot gas from individual supernovae should be able to escape.

Consider the evolution of a star that will eventually explode as a supernova. If it is a low mass star in a binary system, it will eventually explode when accretion from its binary partner pushes it beyond the Chandrasekhar limit. Its preexplosion lifetime is so long that the star is no longer in the original molecular cloud in which it was born. Hence it is likely that SN of this type explode in the more tenuous and hot component of the interstellar medium.

On the other hand, if the star is very massive it will plausibly explode while still inside the molecular cloud and so may dissipate all its energy within the molecular cloud. We assume that most stars explode sufficiently close to the surface of the molecular cloud so that the wind bubble produced by the massive star during its main-sequence lifetime and the subsequent supernova explosion causes it to "break out" into the region of the tenuous component of the interstellar medium as well. Using then the simple approach of Cox (1972) for the evolution of a supernova explosion we shall estimate what the time t_{SN} between supernova explosions in a volume V has to be, in order to make consecutive neighbouring supernova shells touch before they dissipate their energy by cooling. We thus obtain (using a cooling coefficient of 4×10^{-23} ergs cm^3 s^{-1} obtained from detailed modeling, Schmutzler 1987, for a temperature of ~ 9 keV):

$$t_{SN} \lesssim 2.8 \times 10^2 \left(\frac{10^7 \text{ pc}^3}{V}\right)\left(\frac{E_{SN}}{10^{51} \text{ ergs}}\right)\left(\frac{n_0}{\text{cm}^{-3}}\right)^{-2} \text{ yr}, \quad (1)$$

where E_{SN} is the energy of the supernova and n_0 the density of the tenuous interstellar medium. A supernova frequency of $1/t_{SN}$ over a time scale much larger than t_{SN} corresponds to a volume filling factor close to unity for the hot remnants, as shown by McKee and Ostriker (1977; their eq. [1]). As long as $n_0 \lesssim 10$ cm^{-3}, t_{SN} is larger than the supernova interval of 1–3 yr (with an uncertainty of a factor of 3) as derived from radio source arguments. In the reverse case, that a star explodes deep inside a molecular cloud, it appears likely that all energy is dissipated inside, and that we can observe only little trace of the event.

Given the scenario described above, it is of interest to consider whether the SN gas is still hot enough to actually give 9^{+9}_{-4} keV: we require the SN shells to touch before the temperature drops below 6×10^7 K–2.2×10^8 K. This corresponds to a maximum time t after the explosion given by

$$t \lesssim 600 \text{ yr} \left(\frac{E_{SN}/10^{51} \text{ ergs}}{n_0/\text{cm}^{-3}}\right)^{1/3}\left(\frac{10^8 \text{ K}}{T}\right)^{5/6}. \quad (2)$$

Putting this time now into the condition for touching between SNRs we obtain the more stringent condition

$$t_{SN} \lesssim 0.02 \text{ yr} \left(\frac{10^7 \text{ pc}^3}{V}\right)\left(\frac{E_{SN}/10^{51} \text{ ergs}}{n_0/\text{cm}^{-3}}\right)^{4/3}\left(\frac{10^8 \text{ K}}{T}\right)^{11/6}, \quad (3)$$

which is in agreement with our estimated range for t_{SN} of 1–3 yr (Kronberg, Biermann, and Schwab 1985) if the temperature is less than about 10^7 K (~ 1 keV) for $n_0 \simeq 1$ cm^{-3}, or $n_0 \simeq 0.05$ cm^{-3} for $T \sim 10^8$ K; interestingly, at both extremes the pressure is not far from $\sim 10^{-9}$ dyn cm^{-3} as determined from radio observations and minimum energy arguments. We note, in addition, that at a temperature of $\sim 10^8$ K, 10^{51} ergs of explosion energy corresponds to about 10 $M_\odot$ (thermal and kinetic energy), so that these temperatures and time scales correspond to the very early Sedov phase (Cox 1972), when the swept-up mass begins to dominate over the ejected mass.

On the other hand, the ambient pressure around the supernovae in M82 may often be so high, that we have to consider the possibility that the SN expansions stop altogether and reach an equilibrium radius *before* cooling sets in. In this case Cox's (1972) analysis is not applicable. With an experimentally estimated $P_0 \simeq 10^{-9}$ dyn cm^{-2} for the external pressure (from radio observations and minimum energy arguments; Kronberg, Biermann, and Schwab 1985, see below), and using the parametrization of McKee and Ostriker (1977) of Chevalier's (1974) shell expansion calculations, we obtain a different condition for t_{SN} which now yields

$$t_{SN} < 16 \text{ yr} \left(\frac{10^7 \text{ pc}^3}{V}\right)\left(\frac{E_{SN}}{10^{51} \text{ ergs}}\right)^{1.27} \frac{1}{(n_0/\text{cm}^{-3})^{0.21}} \times \left(\frac{10^{-9} \text{ dyn cm}^{-2}}{P_0}\right)^{1.24}. \quad (4)$$

Scaling to the density of $\sim 0.27 f_{0.1}{}^{-1/2}$ cm^{-3} and pressure of $\sim 7 \times 10^{-9} f_{0.1}{}^{-1/2}$ dyn cm^{-2} estimated from X-ray observations above, the time scale in equation (4) changes to $2 f_{0.1}{}^{0.7}$ yr, or 10 yr for a filling factor of order unity. This condition appears readily fulfilled. Since we estimate t_{SN} to be of order 1–3 yr, in this case the equilibrium radius is actually never reached because the SN bubbles merge before they reach it. The equilibrium radius itself is

$$R_E = 15 \text{ pc} \left(\frac{E_{SN}}{10^{51} \text{ ergs}}\right)^{0.32} \frac{1}{(n_0/\text{cm}^{-3})^{0.16}} \times \left(\frac{10^{-9} \text{ dyn cm}^{-2}}{P_0}\right)^{0.20}, \quad (5)$$

and so we require that all SN bubbles observed should be noticeably smaller than this in most cases. This is also necessary to reproduce the high temperature indicated by the X-ray spectrum, because at the equilibrium radius cooling becomes important.

At the adopted distance to M82 of 3.25 Mpc, this size corresponds to a diameter of 0".95. The most detailed radio maps currently available of the M82 starburst region (Kronberg, Biermann, and Schwab 1981, 1985; Bartel *et al.* 1987) appear to give good observational confirmation that the supernova remnant candidates in M82 are typically smaller than the expected R_E values given by relation (5).

In summary, the observation of the X-ray plumes outside of the disk of M82 is consistent with the supernova rate which is implied by the radio source population in the nuclear region. The additional effect of heating the interstellar gas by a direct collision with gas from another galaxy is clearly not required to explain the observations (Harwit *et al.* 1987). It seems plausible that an extensive tunnel network, as originally proposed for our galaxy by Cox and Smith (1974), can be established by supernova explosions. Conditions are thus ripe for a major blowout from the disk. Our conclusion has important implica-

tions for all starburst regions, in that it makes it likely that *blowouts should be a common phenomenon* (cf. also Chevalier and Clegg 1985; McCarthy, Heckman, and van Breugel 1987; and Heckman, Armus, and Miley 1987) wherever starburst activity achieves the local threshold conditions discussed here. Even if the volume of the starburst region is much smaller, such as might be the case in the very small active region of a more normal spiral galaxy, ejection of gas would seem to be an expected phenomenon.

b) Inverse Compton Emission

Since we can now estimate the spatial extent of the FIR emission with the *IRAS* satellite data and also with new 1.3 mm data, and other high-frequency radio observations (Klein, Wielebinski, and Morsi 1988), it is worthwhile to reexamine the discussion by Rieke *et al.* (1980) of the possible role of the inverse Compton process in M82's X-ray emission. Inverse Compton X-ray emission could result from the scattering of the FIR photons off the relativistic electrons which produce the radio emission.

We have to compare the range of Lorentz factors, $300 < \gamma < 1000$, required to produce the X-ray emission from the FIR photons, with those of the relativistic electrons. If we assume a minimum total energy for the synchrotron-emitting gas, the minimum-energy magnetic field strength is of order 10^{-4} G, which indeed implies a similar, possibly larger range of Lorentz factors for the relativistic electrons.

Watson, Stanger, and Griffiths (1984) make the important point that the radio and X-ray emission have a very different morphology (see also Kronberg, Biermann, and Schwab 1985). The X-ray emission is strongly extended perpendicular to the disk (see Figs. 1 and 2), while the radio emission is confined to the disk. However, high-frequency radio maps (Klein, Wielebinski, and Morsi 1988) demonstrate that there is actually quite extensive radio emission outside the disk of M82 which, on the other hand, might be partially thermal. Furthermore, there is *no a priori reason to believe that the FIR photon field closely resembles the magnetic field distribution.* We conclude that a detailed discussion of the contribution of inverse Compton emission is worthwhile and now proceed to go through the argument.

Writing the relativistic electron energy distribution per unit volume as $n_{0r}\gamma^{-2.4}\,d\gamma$ in the range γ_1 to γ_2, and ϵ_e for its total energy density, we obtain for the inverse Compton luminosity (cf. Rybicki and Lightman 1979)

$$L_{\rm IC} = \frac{8}{9}\,\sigma_{\rm T} R_{\rm IC} L_{\rm IR} \frac{\epsilon_e}{mc^2}\,\gamma_2{}^{0.6}\gamma_1{}^{0.4}\,, \qquad (6)$$

where $\sigma_{\rm T}$, $R_{\rm IC}$, $L_{\rm IR}$, and mc^2 are, respectively, the Thomson cross section, the thickness of the disk, the far-infrared luminosity, and the rest mass energy of the electron. $L_{\rm IR}$ is 4×10^{10} $L_\odot$ (Rieke *et al.* 1980). We have used the approximation $\gamma_1 \ll \gamma_2$. We note that the upper Lorentz factor γ_2 refers to the energy band in which we observe inverse Compon X-ray emission while the lower Lorentz factor γ_1 enters from the normalization of ϵ_e. This means that we have to use $\gamma_2 \simeq 10^3$. ϵ_e can only be estimated from minimum energy considerations. To do this, we use the radio data of Kronberg *et al.* (1985) and the assumption (Bell 1978*a*, *b*) that protons and electrons have the same energy density when integrated over their entire range of relativistic energies. We thus obtain for $\epsilon_e \simeq 3 \times 10^{-10}$ ergs cm^{-3} (with Miley's [1980] nomenclature: $k = 1$, $\eta = 1$, $z \simeq 0$, $\theta_x = 30''$, $\theta_y = 5''$, $s = 0.2$ kpc, $F_0 = 1.5$ Jy, $\nu_0 = 5$ GHz, $\nu_1 = 0.01$ GHz, $\nu_2 = 100$ GHz, $\langle \sin^{3/2}\,\phi \rangle = 0.36$). $\nu_1 = 0.01$ GHz corresponds to $\gamma_1 \simeq 150$, and so we should use this value for γ_1 in the expression for the inverse Compton emission. To estimate $R_{\rm IC}$, the thickness of the disk, we use the *IRAS* data (*IRAS Small Scale Structure Catalogue;* Helou and Walker 1986) which, for the FIR size of M82, give about 1′, which corresponds to 1 kpc. We can also use 1.3 mm observations of M82 made by R. Chini *et al.* (1986, private communication) with the new 30 mm telescope on Pico Veleta (Spain) which have enough spatial resolution to provide a real map: in this map we recognize the peak of emission (cold dust) around the radio soure 41.9+58 (see Kronberg, Biermann, and Schwab 1985) and a disk of emission of 20″ by 40″; some questions on the exact spatial extent remain because the chopping throw was only 30″ during these observations and so the 20″ thickness measured for the disk may be an underestimate. As a lower limit to the thickness of the disk we will use 30″ for $R_{\rm IC}$ which corresponds to about 300 pc (at our adopted distance of 3.25 Mpc). Putting all these numbers together yields an expected IC X-ray luminosity in the band 1.4–8.9 keV of 1.5×10^{40} ergs s^{-1}, almost half the observed luminosity. The distribution of this emission should extend at least as far as the far-infrared emission. The most uncertain number entering the estimated inverse Compton X-ray emission is γ_1 which might be very much lower. Had we used, for instance, $\nu_1 = 10^{-3}$ GHz instead of 10^{-2} GHz, then $\epsilon_e \simeq 4 \times 10^{-9}$ ergs cm^{-3}. However, γ_1 and γ_2 are reduced and thus compensate for the increase of ϵ_e in equation (6). So our estimate for $L_{\rm IC}$ is slightly reduced to 1.2×10^{40} ergs s^{-1}. On the other hand, the scale $R_{\rm IC}$ may be much larger, since an infrared emitting disk fills a nearly spherical volume of infrared photons of a diameter equal to the disk diameter. In other words, the IC-emitting volume may extend further above the M82 FIR-emitting volume.

We conclude that inverse Compton scattering of relativistic electrons and far-infrared thermal photons may provide a considerable part of the entire X-ray luminosity beyond the soft energy band. It is, however, less likely to be relevant at large off-axis distances from M82's nucleus. Here free-free emission is more likely to dominate.

IV. SUMMARY

We have presented the most accurate X-ray spectrum yet of a starburst galaxy.

The X-ray data combined with the radio observations (Kronberg, Biermann, and Schwab 1981, 1985) strongly support the concept of a major blowout from the disk driven by the energy release from young stars and their supernova explosions. Such blowouts are likely to be a common phenomenon in starburst galaxies.

We suggest that the observed X-ray emission is most likely a combination of inverse Compton and thermal radiation in which the former is more prominent near the central parts of the galaxy.

Detailed mapping of M82 in the millimeter and submillimeter range will provide the required spatial resolution to model the FIR radiation and to constrain the contribution from inverse Compton emission to the observed X-ray radiation. A final judgement on this point cannot be made with the data presently available.

The authors thank the staff of the *EXOSAT Observatory* for their support during the observations and their help with the

data reduction. We thank Dr. B. Aschenbach for his generous help with the final analysis of the LE data and Dr. P. Müller for supplying the background observation. We especially thank Dr. P. Barr for sharing with us the details of the M81 observations conducted by him and Dr. P. Giommi. We also wish to thank Dr. F. D. Seward for sending us all the MPC data, as well as the data of the serendipitous HRI observation of M82, Dr. H. C. Arp for the use of his [O II] photo, and Dr. R. Wielebinski and Dr. R. Chini for letting us use their high-frequency and millimeter maps of M82. Finally, we wish to acknowledge useful and detailed comments by Dr. C. Henkel and the referee.

REFERENCES

Allen, C. W. 1973, *Astrophysical Quantities* (3d ed.; London: Athlone).
Barr, P., and Giommi, P. 1985*a*, *IAU Circ.*, No. 4044.
———. 1985*b*, private communication.
Bartel, N., *et al.* 1987, *Ap. J.*, **323**, 505.
Bell, A. R. 1978*a*, *M.N.R.A.S.*, **188**, 147.
———. 1978*b*, *M.N.R.A.S.*, **188**, 443.
Chevalier, R. A. 1974, *Ap. J.*, **188**, 501.
Chevalier, R. A., and Clegg, A. W. 1985, *Nature*, **317**, 44.
Cox, D. P. 1972, *Ap. J.*, **178**, 159.
Cox, D. P., and Smith, B. W. 1974, *Ap. J. (Letters)*, **189**, L105.
de Korte, P. A. J., *et al.* 1981, *Space Sci. Rev*, **30**, 495.
Elvis, M., and van Speybroeck, L. 1982, *Ap. J. (Letters)*, **257**, L51.
Fabbiano, G. 1988, *Ap. J.*, **330**, 672.
Harwit, M., Houck, J. R., Soifer, B. T., and Palumbo, G. G. C. 1987, *Ap. J.*, **315**, 28.
Heckman, T. M., Armus, L., and Miley, G. K. 1987, *A.J.*, **92**, 276.
Helou, G., and Walker, D. W. 1986, *IRAS Small Scale Structure Catalogue* (Pasadena: Jet Propulsion Laboratory).
Klein, U., Wielebinski, R., and Morsi, H. W. 1988, *Astr. Ap.*, **190**, 41.
Kronberg, P. P., Biermann, P., and Schwab, F. R. 1981, *Ap. J.*, **246**, 751.
———. 1985, *Ap. J.*, **291**, 693.
Kronberg, P. P., and Sramek, R. A. 1985, *Science*, **227**, 28.
McCarthy, P. J., Heckman, T., and van Breugel, W. 1987, *A.J.*, **92**, 264.
McKee, C. F., and Ostriker, J. P. 1977, *Ap. J.*, **218**, 148.
Miley, G. 1980, *Ann. Rev. Astr. Ap.*, **18**, 165.
Rieke, G. H., Lebofsky, M. J., Thompson, R. I., Low, F. J., and Tokunaga, A. T. 1980, *Ap. J.*, **238**, 24.
Rybicki, G. B., and Lightman, A. P. 1979, *Radiative Processes in Astrophysics* (New York: Wiley).
Schmutzler, T. 1987, Ph.D. thesis, Bonn University.
Sofue, Y., Handa, T., Hayashi, M., and Nakai, N. 1986, preprint.
Soifer, B. T., Sanders, D. B., Neugebauer, G., Danielson, G. E., Lonsdale, C. J., Madore, B. F., and Persson, S. E. 1986, *Ap. J. (Letters)*, **303**, L41.
Taylor, B. G., Andresen, R. D., Peacock, A., and Zobl, R. 1981, *Space Sci. Rev*, **30**, 479.
Turner, M. J. L., Smith, A., and Zimmermann, H. U. 1981, *Space Sci. Rev.*, **30**, 513.
Watson, M. G., Stanger, V., and Griffiths, R. E. 1984, *Ap. J.*, **286**, 144.

P. L. BIERMANN: Max-Planck-Institut für Radioastronomie, Auf dem Hügel 69, D-5300 Bonn 1, West Germany

P. P. KRONBERG: University of Toronto, Department of Astronomy, 60 St. George Street, Toronto, Ontario M5S 1A7, Canada

W. PIETSCH: Max-Planck-Institut für Physik und Astrophysik, Institut für extraterrestrische Physik, D-8046 Garching, West Germany

R. SCHAAF: Astronomische Institute der Universität Bonn, Auf dem Hügel 71, D-5300 Bonn 1, West Germany

T. SCHMUTZLER: Max-Planck-Institut für Kernphysik, Saupfercheckweg 1, D-6900 Heidelberg 1, West Germany